JOURNAL OF THE INSTITUTION OF ENGINEERS (INDIA)", VOL. 88, SEPTEMBER 2007, Pages: 45-51.

Input-Output Linearizing and Decoupling Control of an Induction Motor Drive

Dr K B Mohanty, ***Member*** kbmohanty@nitrkl.ac.in, barada5@rediffmail.com

This paper presents an input-output linearizing and decoupling control scheme for speed control of an induction motor drive. In this scheme, the motor model is linearized, and torque and flux are decoupled by use of nonlinear control along with proportional-cum-integral controllers. The control scheme is implemented and tested in laboratory.

Keywords : Induction motor drive; Input-output linearizing control; Decoupling control; Flux estimation; Slip speed control

NOTATIONS

G: the flux observer gain matrix

$\boldsymbol{i}_{dqr} = [i_{dr}, \; i_{qr}]^T = i_{dr} - j\, i_{qr}$: the rotor current vector

$\boldsymbol{i}_{dqs} = [i_{ds}, \; i_{qs}]^T = i_{ds} - j\, i_{qs}$: the stator current, in real vector notation (former), or in complex vector notation (later)

$\mathrm{I} = \begin{bmatrix} 1 & 0 \\ 0 & 1 \end{bmatrix}$ and $\mathrm{J} = \begin{bmatrix} 0 & -1 \\ 1 & 0 \end{bmatrix}$

P : number of pole pairs

R_s, R_r : stator and rotor resistance per phase respectively

$\boldsymbol{v}_{dqs} = [v_{ds}, \; v_{qs}]^T = v_{ds} - j\, v_{qs}$: the stator voltage vectors

ω_e, ω_r : angular electrical speed of the reference frame and speed of rotor, respectively

$\Psi_{dqr} = [\psi_{dr}, \; \psi_{qr}]^T = \psi_{dr} - j\, \psi_{qr}$: the rotor flux linkage vector

$\Psi_{dqs} = [\psi_{ds}, \; \psi_{qs}]^T = \psi_{ds} - j\, \psi_{qs}$: the stator flux linkage vector

$\hat{\Psi}_{dqr}$: the estimated rotor flux

Dr K B Mohanty is with the Department of Electrical Enginerring, NIT Rourkela 769008.

This paper was received on August 19, 2004. Written discussion on the paper will be entertained till November 30, 2007.

INTRODUCTION

One significant development in induction motor control over last three decades is the field oriented or vector control[1]. In vector control the torque and flux are decoupled by a suitable decoupling network. Then the flux component and the torque component (at quadrature to flux component) of the stator current, or in other words, the amplitude and phase angle of the stator current are controlled independently to control the induction motor (IM) as a separately excited DC motor. Though good dynamic current (or torque) and speed responses are obtained with conventional vector control, the torque is only asymptotically decoupled from the flux, i.e., decoupling is obtained only in steady state, when the flux amplitude is constant. Coupling is still present, when flux is weakened in order to operate the motor at higher speed within the input voltage saturation limits[1], or when flux is adjusted in order to maximize power efficiency[2]. This has led to further research on application of differential geometry[3-4] to develop the control techniques for linearization and decoupling control. A current command input-output linearization controller is reported[2], where the IM drive is controlled for good dynamic performance and maximum power efficiency by linear decoupling of rotor flux and torque. On the basis of steady state errors, rotor resistance errors are computed and used in the output feedback control algorithm in order to reduce the errors. Differential geometry is also applied[5], to linearize the induction motor in field oriented coordinates. The decoupling of torque and flux is achieved by a static state feedback controller. The decoupling of torque and flux, using the amplitude and frequency of the supply voltage as inputs, is also obtained by a static state feedback controller[6] and by a dynamic state feedback controller[7]. Only the electromagnetic part is modeled, and mechanical dynamics is neglected in that study. Marino, *et al*[8] have developed a voltage command input-output linearizing and decoupling controller for the induction motor drive. The linearizing controller is made adaptive to parameter variations. Linearizing control theory is applied to IM control[9], after adding an integrator to one of the inputs. A globally stable

controller is presented[10], for torque regulation of an induction motor with partial state feedback. Input-output linearizing control theory is also applied to IM drive[11-12]. In this paper, a new approach for input-output linearization and decoupling control of induction motor is discussed and a speed adaptive flux observer is designed. Simulation and experimental results are presented and discussed at the end.

LINEARIZING AND DECOUPLING CONTROL

A basic understanding of the decoupled flux and torque control resulting from field orientation or input-output linearization can be attained from the d-q axis model of an induction motor (IM) with the reference axis rotating at synchronous speed, ω_e. The voltage equations of the IM in this synchronously rotating reference frame[13] are:

$$\boldsymbol{v}_{dqs} = R_s \boldsymbol{i}_{dqs} + \dot{\Psi}_{dqs} + \omega_e \mathrm{J}\, \Psi_{dqs} \quad (1)$$

$$0 = R_r \boldsymbol{i}_{dqr} + \dot{\Psi}_{dqr} + (\omega_e - P\omega_r)\mathrm{J}\, \Psi_{dqr} \quad (2)$$

A state variable model of the induction motor with stator current and rotor flux vectors as state variables is obtained by simplification of equations (1-2) along with the flux-linkage equations[13]. The model is as follows:

$$\dot{\boldsymbol{i}}_{dqs} = (-a_1\mathrm{I} - \omega_e\mathrm{J})\boldsymbol{i}_{dqs} + (a_2\mathrm{I} - Pa_3\omega_r\mathrm{J})\Psi_{dqr} + c\boldsymbol{v}_{dqs} \quad (3)$$

$$\dot{\Psi}_{dqr} = a_5 \boldsymbol{i}_{dqs} + \{-a_4\mathrm{I} - (\omega_e - P\omega_r)\mathrm{J}\}\Psi_{dqr} \quad (4)$$

where $c = \dfrac{L_r}{L_s L_r - L_m^2}$; $a_1 = c R_s + \dfrac{c R_r L_m^2}{L_r^2}$;

$a_2 = \dfrac{c R_r L_m}{L_r^2}$; $a_3 = \dfrac{c L_m}{L_r}$; $a_4 = \dfrac{R_r}{L_r}$; and

$a_5 = \dfrac{R_r L_m}{L_r}$

The field orientation concept implies that the current components supplied to the motor should be oriented in phase (flux component) and in quadrature (torque component) to the rotor flux vector Ψ_{dqr}. This can be accomplished by choosing the speed of the reference frame ω_e to be the instantaneous speed of Ψ_{dqr} and locking the phase of the reference system such that the rotor flux is entirely in the *d*-axis (flux axis). This results in the mathematical constraint:

$$\psi_{qr} = 0 \text{ and } \dot{\psi}_{qr} = 0 \quad (5)$$

To achieve equation (5) the constraint on the synchronous speed is as follows: (obtained from (4))

$$\omega_e = P\omega_r + a_5 i_{qs} / \psi_{dr} \quad (6)$$

When equation (5) is satisfied, the dynamic behavior of the induction motor is:

$$\dot{i}_{ds} = -a_1 i_{ds} + a_2 \psi_{dr} + \omega_e i_{qs} + c v_{ds} \quad (7)$$

$$\dot{i}_{qs} = -\omega_e i_{ds} - a_1 i_{qs} - P a_3 \omega_r \psi_{dr} + c v_{qs} \quad (8)$$

$$\dot{\psi}_{dr} = -a_4 \psi_{dr} + a_5 i_{ds} \quad (9)$$

The torque developed by the induction motor is:

$$T_e = K_t \psi_{dr} i_{qs} \quad (10)$$

where $K_t = \dfrac{3 P L_m}{2 L_r}$ is the torque constant.

The field oriented induction motor model, described by equation (7) to equation (10), has nonlinearity. The speed emf term ($\omega_r \psi_{dr}$) appearing in (8) makes the current dynamics nonlinear and speed dependent. Equation (7) and equation (8) show that interaction between current components does exist, in the rotating reference frame. The transition from field oriented voltage components, v_{ds} and v_{qs} to current components as in equation (7) and equation (8) involves leakage time constants and interactions. During the flux transient period (equation (9)) coupling of flux and torque is obvious from equation (7) to equation (10). The interaction between current components, and nonlinearity in the overall system are eliminated by using input-output linearization and decoupling control[2, 5, 8, 12]. The present approach consists of change of coordinates and use of nonlinear inputs to linearize the system equations. Developed torque T_e is considered as a state variable, replacing i_{qs} to describe the motor dynamics. Using equations (6), (8), (9), and (10), the torque dynamic equation is expressed as:

$$\dot{T}_e = -(a_1 + a_4)T_e + K_t \psi_{dr}\left[c v_{qs} - P\omega_r (i_{ds} + a_3 \psi_{dr})\right] \quad (11)$$

The nonlinearities in equation (7) and equation (11) are put together and then replaced by nonlinear functions of the form u_1 and u_2 respectively. Equation (7) and equation (11) are then modified as follows.

$$\dot{i}_{ds} = -a_1 i_{ds} + a_2 \psi_{dr} + u_1 \quad (12)$$

$$\dot{T}_e = -(a_1 + a_4) T_e + u_2 \quad (13)$$

With these linearizing inputs u_1 and u_2, the flux and torque are decoupled. Controllers are designed to obtain u_1 and u_2, which maintain decoupling and linearization under all conditions. The stator input voltage components v_{ds} and v_{qs} in terms of u_1 and u_2 are:

$$v_{ds} = \frac{(-\omega_e i_{qs} + u_1)}{c} \quad (14)$$

$$v_{qs} = \frac{1}{c}\left[P\omega_r (i_{ds} + a_3 \psi_{dr}) + \frac{u_2}{K_t \psi_{dr}}\right] \quad (15)$$

The block diagram of the induction motor drive with this input-output linearizing control scheme is shown in Figure 1. The design procedure for the P-I controllers is detailed elsewhere[12]. The gains as given there:

K_{p3} = 151.24, K_{i3} = 43640, K_{p1} = 0.26, K_{i1} = 1.98, K_{p2} = 100, K_{i2} = 29877.

ROTOR FLUX ESTIMATION

The input-output linearization and decoupling control algorithm given by equation (6), equation (14) and equation (15) requires the knowledge of rotor flux. However, it is difficult to measure the rotor flux of induction motor, practically. Therefore, the rotor flux is to be estimated from the measured values of speed, stator current and voltage. Gopinath's reduced order observer[14] is applied to estimate the rotor flux. The IM model described by equation (3) and equation (4) is written in the form:

$$\dot{\boldsymbol{i}}_{dqs} = \mathrm{A}_{11}\,\boldsymbol{i}_{dqs} + \mathrm{A}_{12}\,\Psi_{dqr} + \mathrm{B}_1\,\boldsymbol{v}_{dqs} \qquad (16)$$

$$\dot{\Psi}_{dqr} = \mathrm{A}_{21}\,\boldsymbol{i}_{dqs} + \mathrm{A}_{22}\,\Psi_{dqr} \qquad (17)$$

where $\mathrm{A}_{11} = -a_1\,\mathrm{I} - \omega_e\,\mathrm{J}$;

$\mathrm{A}_{12} = a_2\,\mathrm{I} - P\,a_3\,\omega_r\,\mathrm{J}$; $\mathrm{A}_{21} = a_5\,\mathrm{I}$;

$\mathrm{A}_{22} = -a_4\,\mathrm{I} - (\,\omega_e - P\,\omega_r\,)\,\mathrm{J}$; and $\mathrm{B}_1 = c\,\mathrm{I}$

From equation (17), the flux observer equation with an error correction term[14] is derived as follows:

$$\dot{\hat{\Psi}}_{dqr} = \mathrm{A}_{21}\,\boldsymbol{i}_{dqs} + \mathrm{A}_{22}\,\hat{\Psi}_{dqr} + \mathrm{G}\left[\dot{\boldsymbol{i}}_{dqs} - (\,\mathrm{A}_{11}\,\boldsymbol{i}_{dqs} + \mathrm{A}_{12}\,\hat{\Psi}_{dqr} + \mathrm{B}_1\,\boldsymbol{v}_{dqs}\,)\right] \qquad (18)$$

Subtracting equation (18) from equation (17), the flux error dynamics for this observer is:

$$\dot{\tilde{\Psi}}_{dqr} = (\,\mathrm{A}_{22} - \mathrm{G}\,\mathrm{A}_{12}\,)\,\tilde{\Psi}_{dqr} \qquad (19)$$

where $\tilde{\Psi}_{dqr} = \Psi_{dqr} - \hat{\Psi}_{dqr}$ is the error in the flux estimate.

It is verified that the matrix pair ($\mathbf{A}_{12}$, $\mathbf{A}_{22}$) is observable for all real ω_r. So, by choosing suitable gain matrix *G*, the eigen-values of the matrix $(\mathrm{A}_{22} - \mathrm{G}\,\mathrm{A}_{12})$ can be placed in the left half of s-plane, so that the estimated flux $\hat{\Psi}_{dqr}$ approaches the actual flux Ψ_{dqr} asymptotically.

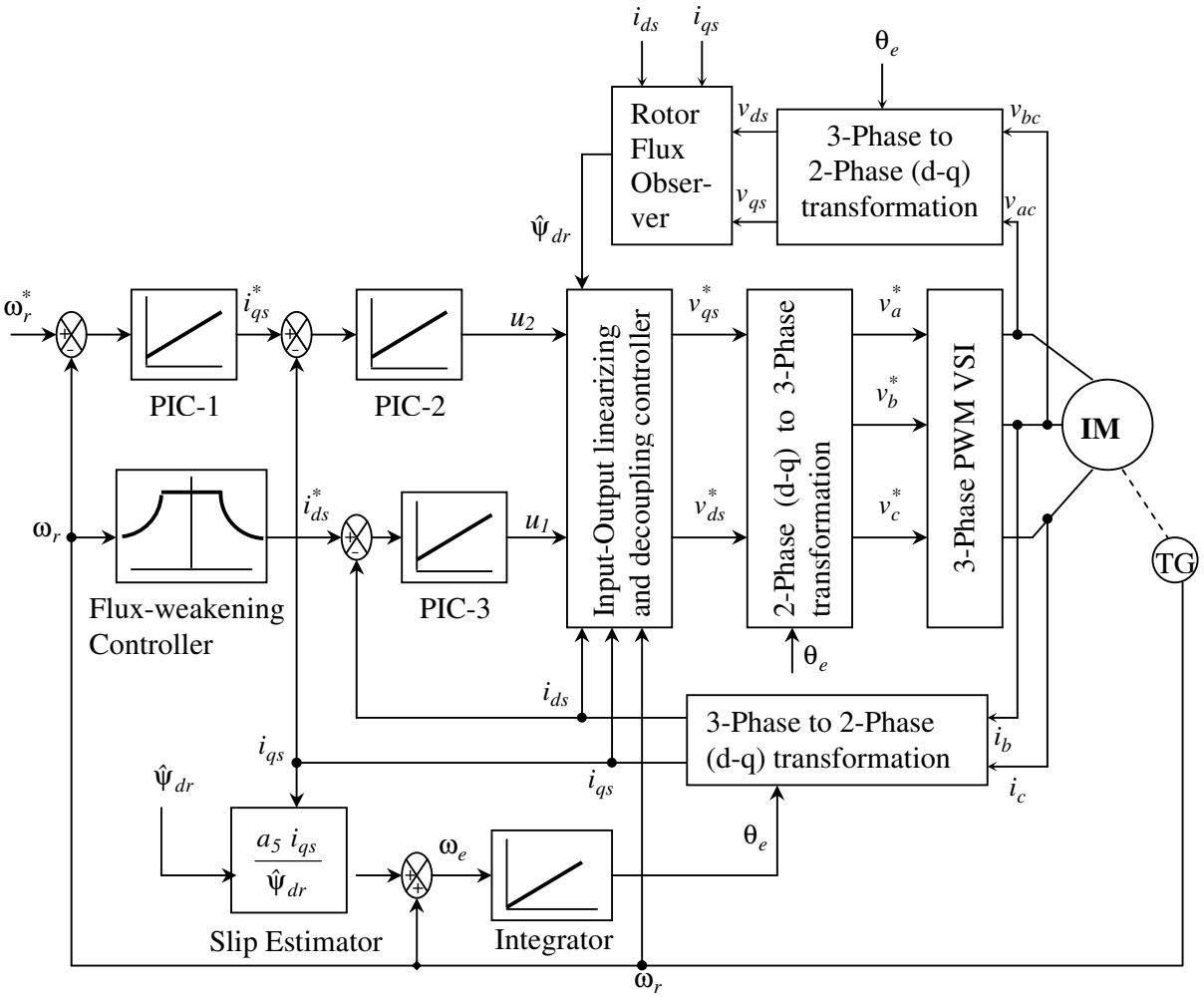

PIC : Proportional-cum-Integral Controller

Figure 1 Schematic diagram of the IM drive with Input-Output linearizing control scheme

It is desirable to eliminate the differential term of the current in equation (18). So a dummy variable defined by equation (20) is chosen. The algorithm for implementing observer equation (18) is as follows:

$$\hat{\boldsymbol{\xi}} = \hat{\Psi}_{dqr} - \mathrm{G}\, \boldsymbol{i}_{dqs} \tag{20}$$

$$\dot{\hat{\boldsymbol{\xi}}} = (\mathrm{A}_{22} - \mathrm{G}\,\mathrm{A}_{12})\hat{\boldsymbol{\xi}} + [\mathrm{A}_{21} - \mathrm{G}\,\mathrm{A}_{11} + (\mathrm{A}_{22} - \mathrm{G}\,\mathrm{A}_{12})\mathrm{G}]\,\boldsymbol{i}_{dqs} - \mathrm{G}\,\mathrm{B}_1\,\boldsymbol{v}_{dqs} \tag{21}$$

To place the eigen-values of the matrix $(\mathrm{A}_{22} - \mathrm{G}\,\mathrm{A}_{12})$ at $(-x \pm j\,y)$ rad/sec, the required observer gain matrix G is given by $(g_1\,\mathrm{I} + g_2\,\mathrm{J})$, where

$$g_1 = \frac{(x - a_4)a_2 + (y + \omega_e - P\,\omega_r)P\,a_3\,\omega_r}{a_2^2 + (P\,a_3\,\omega_r)^2} \tag{22}$$

$$g_2 = \frac{(x - a_4)P\,a_3\,\omega_r - (y + \omega_e - P\,\omega_r)\,a_2}{a_2^2 + (P\,a_3\,\omega_r)^2} \tag{23}$$

Selection of values for x and y is a compromise between sensitivity to measurement error and rapid recovery of initial error. A fast observer converges quickly, but it is also sensitive to measurement error. The rotor flux is estimated by solving for $\hat{\boldsymbol{\xi}}$ from equation (21), and then substituting in equation (20).

EXPERIMENTAL RESULTS AND DISCUSSIONS

The input-output linearization and decoupling controller and flux observer was implemented on an IGBT (Insulated Gate Bipolar Transistor) based PWM inverter fed induction motor drive with the help of a 75 MHz Pentium processor based PC housed with moderately priced add-on cards, such as A/D card (PCL-208) and D/A card (PCL-726) from Dynalog Microsystems, India. The software controller was implemented in C language. Sampling time was fixed at 500 µsec by using 8254 timer of the PC. Once the timer has finished, the interrupt controller calls the channel interrupt, that is used for reading the A/D converter data each 500 µsec. The time required by the PC to execute the control loop once has been found to be 286 µsec approximately. For closed loop control, the motor is initially started on open loop in constant Volts/Hertz mode. After the motor achieves the steady state operation at a desired frequency, the control algorithm is switched on for closed loop operation. The rating and parameters of the 3-phase induction motor used in the experimental study are given in Table 1.

Figure 2 shows the simulated and experimental responses for a step increase in speed reference from 1000 r/min to 1480 r/min with linearizing control.

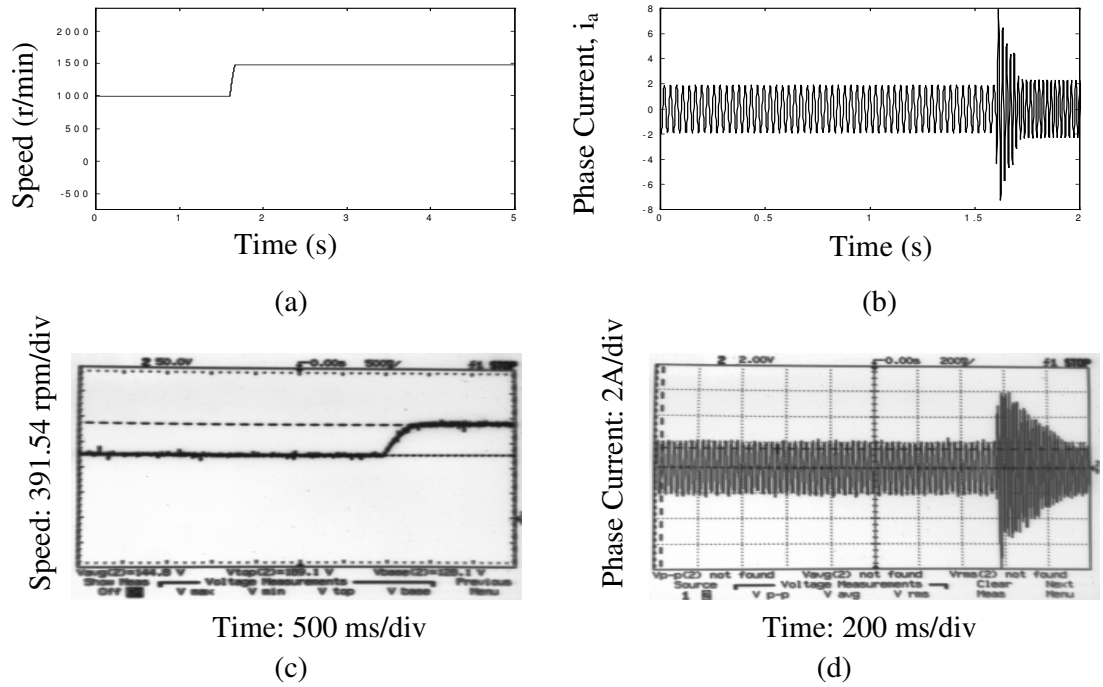

Figure 2 Simulation and experimental responses for step increase in reference speed from 1000 to 1480 r/min (reference flux linkage = 0.45 V.s): (i) Simulation response (a) Speed (b) Phase current; (ii) Experimental response (c) Speed (d) Phase current

There are some differences in the transient responses, though the steady state values are equal. Settling time for current is approximately 260 ms from the experimental result, and 140 ms from the simulation one. Settling time for speed is approximately 300 ms from the experimental result, and 65 ms from the simulation one. The difference in the transient response is due to several factors, such as ceiling in the inverter voltages, inverter nonlinearity, measurement noise, magnetic saturation etc.

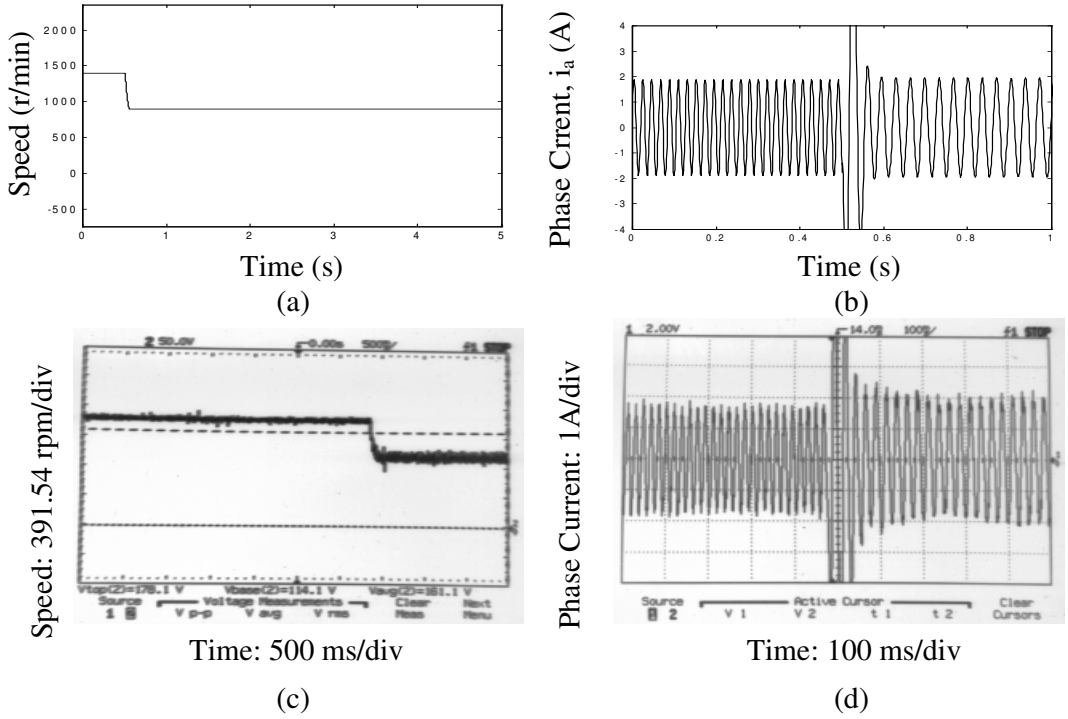

Figure 3 Simulation and experimental responses for step decrease in reference speed from 1400 to 900 r/min (reference flux linkage = 0.45 V.s): (i) Simulation response (a) Speed (b) Phase current; (ii) Experimental response (c) Speed (d) Phase current

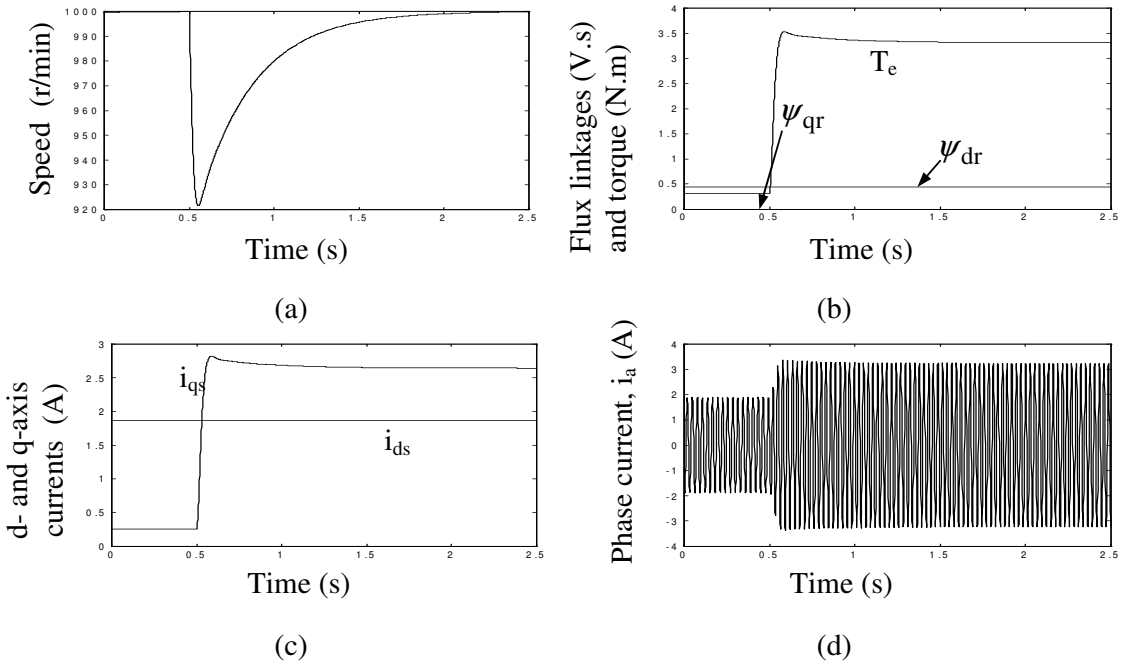

Figure 4 Simulation response for step change in load torque: (a) speed (b) d- and q-axis rotor flux linkages and developed torque (c) d- and q-axis stator currents (d) Stator phase current

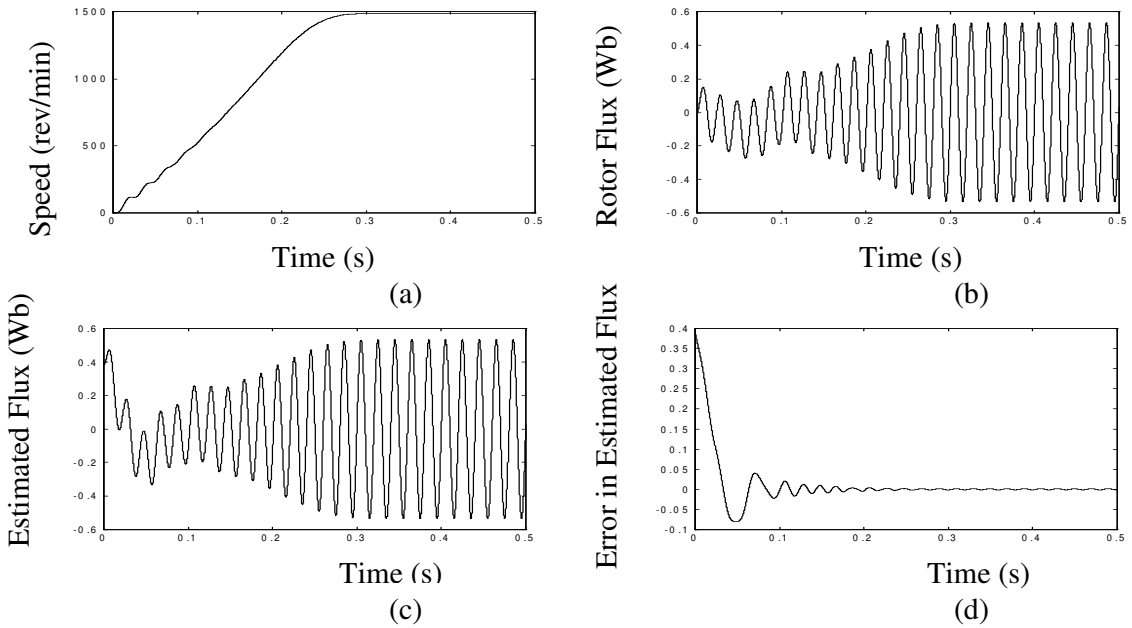

Figure 5 Simulation response with flux observer when staring from standstill (a) Rotor speed (b) Actual rotor flux (c) Estimated rotor flux of observer (d) Flux estimation error

Figure 3 shows the simulated and experimental responses for a step decrease in speed reference from 1400 r/min to 900 r/min. Settling time for current is approximately 220 ms from the experimental result, and 100 ms from the simulation one. Settling time for speed is approximately 200 ms from the experimental result, and 60 ms from the simulation one. Figure 4 shows the simulation response for a step change in load torque from 0 to 3 N·m. Developed torque response exhibits an overshoot of 0.2 N·m (6.67%). The d-axis rotor flux linkage remains constant at 0.45 V·s and q-axis rotor flux linkage remains constant at zero. During the transient period of torque change, speed drops by 78 r/min (7.8%) and settles to 3% of reference value in 0.37 s. Decoupling of torque and flux, or in other words, torque and flux components of stator current is apparent from Figure 4. Figure 5 shows performance of the flux observer. Speed, actual and estimated rotor flux, and flux estimation error from a simulation study, after the motor is started from standstill, are shown.

Table 1 Rating and Parameters of the Induction Motor

Three phase, 50 Hz, 0.75 kW, 220V, 3A, 1440 rpm
Stator and rotor resistances: $R_s = 6.37\ \Omega$, $R_r = 4.3\ \Omega$
Stator and rotor self inductances: $L_s = L_r = 0.26$ H
Mutual inductance between stator and rotor: $L_m = 0.24$ H
Moment of Inertia of motor and load: $J = 0.0088$ Kg ·m^2
Viscous friction coefficient: $\beta = 0.003$ N ·m ·s/rad

CONCLUSIONS

The concept of input-output linearization and decoupling control as applied to the induction motor drive is clearly presented. A speed adaptive reduced order observer for estimation of rotor flux has been developed. The designed controller and flux observer has been implemented in the laboratory, on an IGBT based PWM inverter fed IM drive with the help of a 75 MHz Pentium processor based PC, and tested. The experimental results of the drive are compared with corresponding simulation results. Within the limitations of the experimental set-up, satisfactory agreement is found among them thus validating the control algorithm.

REFERENCES

1. W. Leonhard, *Control of Electrical Drives*, Springer-Verlag: Berlin, Germany, 1990.
2. D. I. Kim, I. J. Ha and M. S. Ko, "Control of induction motors via feedback linearization with input-output decoupling," *Int. Journal of Control*, vol. 51, no. 4, 1990, pp. 863-883.
3. A. Isidori, A. J. Krener, C. Gori-Giorgi, and S. Monaco, "Nonlinear decoupling via feedback: A differential-geometric approach," *IEEE Trans. AC*, vol. 26, 1981, pp. 331-345.
4. T. J. Tarn, A. K. Bejczy, A. Isidori and Y. Chen, "Nonlinear feedback in robot arm control," *Proc. of 23rd Conf. on Decision and Control*, Dec. 1984, pp. 736-751.
5. Z. Krzeminski, "Nonlinear control of induction motor," *Proc. of 10th IFAC World Congress on Automatic Control*, vol. 3, Munich, 1987, pp. 349-354.
6. A. De Luca, and G. Ulivi, "Design of exact nonlinear controller for induction motors," *IEEE*

Trans. AC, vol. 34, no. 12, Dec. 1989, pp 1304-1307.
7. A. De Luca, and G. Ulivi, "Dynamic decoupling of voltage frequency controlled induction motors," 8th Int. Conf. on Analysis and Optimization of Systems, Antibes, June 1988, pp. 127-137.
8. R. Marino, S. Peresada, and P. Valigi, "Adaptive input-output linearizing control of induction motors," *IEEE Trans. AC*, vol. 38, no. 2, 1993, pp. 208-221.
9. J. Chiasson, "Dynamic feedback linearization of the induction motor," *IEEE Trans. AC*, vol. 38, no. 10, Oct. 1993, pp. 1588-1594.
10. R. Ortega and G. Espinosa, "A controller design methodology for systems with physical structures: Applications to induction motors," *Automatica*, vol. 29, no. 3, 1993, pp. 621-633.
11. M. Bodson, J. Chiasson and R. Novotnak, "High perfomance induction motor control via input-output linearization," *IEEE Control Systems Magazine*, Aug. 1994, pp. 25-33.
12. K. B. Mohanty and N. K. De, "Nonlinear controller for induction motor drive," *Proc. of IEEE Int. Conf. on Industrial Technology (ICIT)*, Jan. 2000, Goa, India, pp. 382-387.
13. P. C. Krause, *Analysis of Electrical Machinery,* McGraw-Hill, New York, 1986.
14. Y. Hori, V. Cotter, and Y. Kaya, "Control theoretical considerations relating to an induction machine flux observer," *IEE Proc*., 106-B, 1986, pp. 1001-1008.